Chemical Engineering Journal 162 (2010) 186–193

Contents lists available at ScienceDirect

Chemical Engineering Journal

journal homepage: www.elsevier.com/locate/cej

Removal of heavy metals using polyvinyl alcohol semi-IPN poly(acrylic acid)/tourmaline composite optimized with response surface methodology

Yian Zheng[a,b], Aiqin Wang[a,*]

[a] Center of Eco-materials and Green Chemistry, Lanzhou Institute of Chemical Physics, Chinese Academy of Sciences, Tianshui Middle Road, No. 18, Lanzhou, 730000, PR China
[b] Graduate University of the Chinese Academy of Sciences, Beijing, 100049, PR China

ARTICLE INFO

Article history:
Received 4 October 2009
Received in revised form 6 May 2010
Accepted 10 May 2010

Keywords:
Response surface methodology
Box–Behnken design
Adsorption
Heavy metal
Polyvinyl alcohol

ABSTRACT

The heavy metals, Pb^{2+} and Cu^{2+} adsorption was studied using polyvinyl alcohol semi-IPN poly (acrylic acid)/tourmaline (PVA semi-IPN PAA/Tm) composite as the adsorbent. During the preparation process of adsorbent, response surface methodology (RSM) based on three-variable-three-level Box–Behnken design (BBD) was employed. The effects of three variables, i.e. neutralization degree (ND) of AA, PVA:AA ratio, and Tm:AA ratio on the adsorption capacity for Pb^{2+} and Cu^{2+} (as response) were evaluated. The results indicated that ND of AA and Tm:AA were the most significant preparation variables affecting Pb^{2+} and Cu^{2+} removal. Models capable of predicting the maximum adsorption capacity were established and the optimum preparation conditions were determined as follows: ND of AA, 68–69%, PVA:AA, 0.0973, Tm:AA, 0.20. Under these conditions, the predicted values of models (3.18 mmol/g for Pb^{2+} and 3.00 mmol/g for Cu^{2+}) were in good agreement with experimental results (3.12 mmol/g for Pb^{2+} and 2.98 mmol/g for Cu^{2+}). The adsorption kinetics of as-prepared composite under non-competitive and competitive conditions suggested that the adsorption equilibrium could be achieved within 30 min. In addition, as-prepared composite showed good reusability with 0.1 mol/L EDTA as the desorbing agent, and the adsorption process was mainly controlled by ion exchange and chelation interaction.

1. Introduction

Heavy metal pollution has become one of the serious environmental problems of worldwide concern. Heavy metals released into the environment have been increased continuously as a result of the rapid development of various industrial activities and technologies, posing a direct or indirect threat to environment and public health because of their toxicity and bioaccumulation in the food chain and persistence in nature. The heavy metals like lead, mercury, copper, cadmium, zinc, nickel, chromium are among the most common pollutants found in industrial effluents, and are non-biodegradable and toxic even at low concentration [1]. Consequently, the removal of them from the process or waste effluents becomes environmentally important. Various methods for heavy metal removal, including microbial degradation, bioaccumulation, chemical oxidation, membrane separation, electrochemical treatment, filtration, and reverse osmosis, have been proposed [2]. However, these methods have several disadvantages, such as incomplete metal removal, high reagent and energy requirements and generation of toxic sludge or other waste products that require disposal and further treatment. For heavy metals removal, adsorption is generally preferred due to high efficiency, easy handling, and availability of different adsorbents.

Nowadays, development of new adsorbents having superior properties such as high adsorption capacity and fast adsorption rate has generated great interests for heavy metal removal. Hydrogels are defined as the water-swollen, three-dimensional polymer networks. They can absorb a large amount of water compared with other water absorbing materials. Due to its super-hydrophilicity characteristic, this type of adsorbent shows faster adsorption kinetics for removing heavy metals from the aqueous solution [3,4]. In addition, the surface functionalities of this synthetic polymer can be tailored allowing them to interact with target species [5]. Up to now, acrylic acid (AA) is the most commonly used monomer to obtain the hydrogels [6–8]. Polyvinyl alcohol (PVA) has been a polymer of choice for a long time in biotechnical and biomedical communities. It is used as a basic material for a variety of biomedical applications because of their inherent non-toxicity, non-carcinogenicity, good biocompatibility, and desirable physical properties [9]. By virtue of the excellent hydrophilic characteristics and gelling capability, PVA has been extensively used as water-soluble matrix polymer for preparing IPN and semi-IPN hydrogels [10]. Tourmaline (Tm) belongs to the group of silicate minerals called cyclosilicates. The general chemical formula of the tourmaline group, as a whole, can be expressed as $XY_3Z_6(T_6O_{18})(BO_3)_3V_3W$, where $X = Na^+, Ca^{2+}, K^+$, or vacancy, $Y = Li^+, Fe^{2+}$,

* Corresponding author. Tel.: +86 931 4968118; fax: +86 931 8277088.
E-mail address: aqwang@lzb.ac.cn (A. Wang).

1385-8947/$ – see front matter © 2010 Elsevier B.V. All rights reserved.
doi:10.1016/j.cej.2010.05.027

Mg^{2+}, Fe^{3+}, Al^{3+}, Cr^{3+}, V^{3+}, (Ti^{4+}), Z = Al^{3+}, Fe^{3+}, Mg^{2+}, Cr^{3+}, V^{3+}, (Fe^{2+}), T = Si^{4+}, Al^{3+}, (B^{3+}), B = B^{3+} or vacancy, V = [O(3)] = OH^-, O^{2-}, W = [O(1)] = OH^-, O^{2-}, F^- and metal ions in ( ) indicate minor or possible substitution [11]. Based on above background, a series of hydrogels were prepared using AA as the monomer, PVA as the linear polymer, and Tm as the inorganic component, and subsequently, the adsorption capacities of these hydrogels for heavy metals, Pb^{2+} and Cu^{2+} in this study, were evaluated.

RSM is a statistical method based on the multivariate non-linear model that consists of designing experiments to provide adequate and reliable measurements of the response, developing a mathematical model having the best fit to the data obtained from the experimental design, and determining the optimal value of the independent variables that produces a maximum or minimum response [12–15]. RSM is a powerful tool for statistical modeling using lesser number of experimental runs planned according to experimental design [16]. Now, RSM has been widely used for optimization of the process variables of adsorption [17,18]. However, in these publications, the optimization process is generally performed to investigate the effects of some operating parameters, such as initial pH, temperature, initial adsorbate concentration and adsorbent concentration on the adsorption capacity. In this study, RSM is used to optimize the preparation process of polymeric hydrogels rather than some adsorption parameters, obtaining thus the appropriate preparation conditions with the maximum adsorption capacity for Pb^{2+} and Cu^{2+}. By adopting a three-variable Box–Behnken design (BBD), the following variables were optimized: neutralization degree (ND) of AA, PVA:AA ratio, Tm:AA ratio. Second-order model was used to generate three-dimensional response surfaces of the adsorption capacity for Pb^{2+} and Cu^{2+} ions. The adsorption kinetics experiments were carried out in solutions containing single Pb^{2+} (Cu^{2+}), or complex Pb^{2+} and Cu^{2+} ions using optimum adsorbent. The reusability of as-prepared composite for Pb^{2+} and Cu^{2+} removal was evaluated and the adsorption mechanism was proposed.

2. Experimental

2.1. Materials

Acrylic acid (AA, chemically pure, Sinopharm Chemical Reagent Co., Ltd., Shanghai, China) was distilled under reduced pressure before use. Ammonium persulfate (APS, analytical grade, Sinopharm Chemical Reagent Co., Ltd., Shanghai, China), *N*,*N*′-methylene-bisacrylamide (MBA, chemically pure, Shanghai Yuanfan additives plant, Shanghai, China), polyvinyl alcohol (PVA with the average polymerization degree of 1700 and alcoholysis degree of 99%, Lanzhou Vinylon Factory, Lanzhou, China) were used as received. Tourmaline (Tm, Jinjianshi Nano Technology Co., Ltd., Hebei, China) was milled through a 200-mesh screen prior to use. All other reagents used were of analytical grade and all solutions were prepared with distilled water.

2.2. Preparation of PVA semi-IPN PAA/Tm composite

In a four-neck flask equipped with a stirrer, a condenser, a thermometer and a nitrogen line, an appropriate amount of PVA was dispersed in 60 mL distilled water and heated to 80 °C under stirring until PVA was dissolved completely. Then the temperature was lowed to 70 °C while 4 mL solution containing 0.2 g APS was added dropwise for 10 min. After that, a premixed solution containing 20 mL distilled water, 0.3 g MBA, 7.2 g AA with different ND and an appropriate amount of Tm was added drop by drop from a constant pressure funnel into the reactor. Nitrogen atmosphere was kept throughout the experiments. The solution was stirred at 70 °C for 3 h to complete the polymerization reaction, and the resulting hydrogel was immersed in distilled water to remove any impurities present. The product was dried at 70 °C to a constant weight and the adsorbent used during the adsorption process was milled through a 40–80 mesh screen.

Table 1
Experimental ranges and levels of the independent variables.

Variable	Name	Range and level		
		−1	0	+1
x_1	ND of AA	20	50	80
x_2	PVA:AA	0.0833	0.104	0.125
x_3	Tm:AA	0	0.25	0.50

2.3. Experimental design

The Box–Behnken factorial design was used to optimize the preparation process according to the adsorption capacity of resulting composite for Pb^{2+} and Cu^{2+} ions. The complete design consisted of three levels (low, medium and high coded as −1, 0, and +1) and 17 runs which were preformed in duplicate to optimize the level of chosen variables, i.e. ND of AA, PVA:AA ratio, Tm:AA ratio. For statistical calculations, the three independent variables were designed as X_1, X_2 and X_3, respectively, and were coded according to the following equation:

$$x_i = \frac{X_i - X_0}{\Delta X_i} \quad (1)$$

where x_i is the coded value of an independent variable, X_i is the real value of an independent variable, X_0 is the real value of an independent variable at the centre point and ΔX_i is the step change value [18]. In this study, the experiment design and RSM were employed using Design Expert Software Version 7.1.3 (STAT-EASE Inc., Minneapolis, USA).

The range and levels used in the experiments were listed in Table 1. By the RSM, a quadratic polynomial equation was developed to predict the response as a function of independent variables involving their interactions:

$$Y = \beta_0 + \Sigma\beta_i x_i + \Sigma\beta_{ii} x_i^2 + \Sigma\beta_{ij} x_i x_j \quad (2)$$

where Y is the predicted response; β_0, β_i, β_{ii} and β_{ij} are constant regression coefficient of the model; x_i and x_j ($I = 1 \rightarrow 3$; $j = 1 \rightarrow 3$; $i \neq j$) represent the independent variables in the form of coded values.

The experimental design matrix resulted by the BBD consists of 17 runs in coded terms (Table 2). According to this table, a series of experiments were conducted for obtaining the response, that is, adsorption capacity for Pb^{2+} and Cu^{2+} were carried out at the corresponding independent variables addressed in the experimental design matrix by applying quadratic model.

2.4. Adsorption experiment

Adsorption experiments were carried out by agitating the composite in 25 mL Pb^{2+} or Cu^{2+} ion solution (0.02 mol/L) in a shaker at 30 °C and 120 rpm. The samples were withdrawn from the flasks at predetermined time intervals and analyzed for Pb^{2+} or Cu^{2+} content by EDTA titrimetric method with xylenol orange as the indicator. The adsorption capacity of the composite for Pb^{2+} or Cu^{2+} was calculated through the following equation:

$$q = \frac{(C_0 - C_e)V}{m} \quad (3)$$

where q is the amount of Pb^{2+} or Cu^{2+} adsorbed at time t or at equilibrium (mmol/g), C_0 and C_e is the initial and final concentration of

Table 2
BBD matrix in coded terms along with experimental and predicted values.

Run	Variables (coded)			Pb^{2+} adsorbed (mmol/g)		Cu^{2+} adsorbed (mmol/g)	
	x_1	x_2	x_3	Experimental	Predicted	Experimental	Predicted
1	0	1	−1	2.70	2.97	2.06	2.07
2	1	0	1	2.53	2.42	1.71	1.73
3	1	1	0	2.87	2.83	2.35	2.27
4	0	0	0	2.95	2.95	2.87	2.87
5	−1	1	0	2.86	2.48	1.79	1.80
6	0	0	0	2.95	2.95	2.87	2.87
7	0	−1	1	2.65	2.38	1.56	1.54
8	0	0	0	2.95	2.95	2.87	2.87
9	0	1	1	2.09	2.24	1.56	1.62
10	0	−1	−1	2.69	2.54	2.11	2.05
11	−1	−1	0	1.73	1.77	1.12	1.20
12	−1	0	1	1.48	1.71	0.81	0.74
13	1	−1	0	2.89	3.27	2.77	2.77
14	0	0	0	2.95	2.95	2.87	2.87
15	−1	0	−1	1.84	1.95	1.21	1.19
16	0	0	0	2.95	2.95	2.87	2.87
17	1	0	−1	3.30	3.07	2.17	2.24

Pb^{2+} or Cu^{2+} (mol/L), V is the volume of Pb^{2+} or Cu^{2+} solution used (mL) and m is the mass of the composite used (g).

Furthermore, the composite was also added into the solution containing an equimolar amount (0.01 mol/L) of Pb^{2+} and Cu^{2+} ions to determine the metal ion adsorption capacity under competitive conditions. The residual amount of Pb^{2+} and Cu^{2+} ions were measured for various time intervals and the adsorption capacity were then obtained. In this study, the total adsorption capacity for Pb^{2+} and Cu^{2+} was obtained using EDTA titrimetric method, and then the Cu^{2+} ion was masked with thiourea to determine the adsorption capacity for Pb^{2+} ion. The adsorption capacity for Cu^{2+} ion was achieved by subtracting the adsorption capacity for Pb^{2+} from the total adsorption capacity.

2.5. Desorption and regeneration studies

The desorption of metal ions loaded on the composite was done using 0.1 mol/L HCl or EDTA as the desorbing agent. A fixed amount (50 mg) of each adsorbent was contacted separately with 25 mL 0.1 mol/L HCl or EDTA solution. The bottle was placed in a thermostatic shaker for 60 min at 120 rpm. At the end of the experiment, the supernatant was discarded and the solid was washed with distilled water for several times. Then, the recovered composite was employed for another adsorption. A similar procedure was repeated and the reusability of as-prepared adsorbent was then evaluated.

2.6. Characterization

FTIR was conducted on the Thermo Nicolet NEXUS TM spectrophotometer using KBr pellets. The thermal behaviors of PVA, PAA/Tm and PVA semi-IPN PAA/Tm were evaluated on a Perkin Elmer DSC instrument at a heating rate of 10 °C/min using dry nitrogen purge at a flow rate of 200 mL/min. The surface morphologies of the samples were examined using a JSM-5600 scanning electron microscope (SEM) with gold film.

3. Results and discussion

3.1. FTIR analysis

Fig. 1 shows the FTIR spectra of PVA (a), PVA semi-IPN PAA/Tm (b) and Tm (c). As shown in Fig. 1a, PVA shows an absorption band at 1453 cm^{-1} which is assigned to be a superposition of CH_2 bending and O–H deformation [19]. The perpendicular band at 1340 cm^{-1} should also be related to the hydroxyl group, which

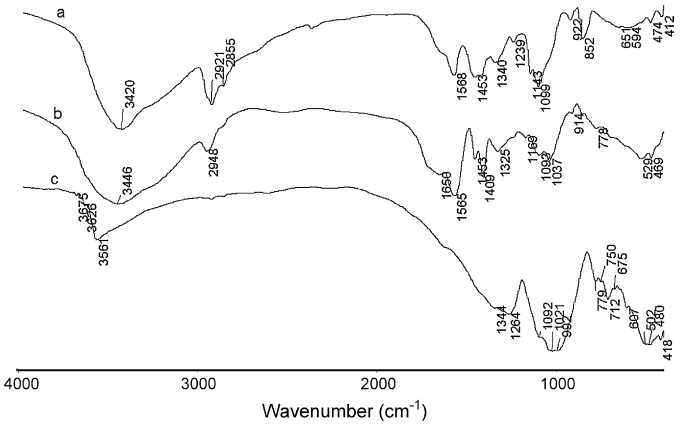

Fig. 1. Infrared spectra of (a) PVA, (b) PVA semi-IPN PAA/Tm, and (c) Tm.

shifts to 1325 cm^{-1} due to the hydrogen bonding between PVA and PAA chains. An important absorption band is verified at a frequency of 1143 cm^{-1}, and this vibrational band is mostly attributed to the crystallization of PVA, related to carboxyl stretching band C–O. Such absorption band at 1143 cm^{-1} has been used as an assessment tool of PVA structure [20,21]. After the reaction, this absorption band disappears, but other absorption bands can still be observed in the composite (Fig. 1b). This gives direct evidence that the linear PVA combines with PAA/Tm hydrogel network by hydrogen bonding interaction and occurs within the hydrogel in the form of semi-IPN, by which the crystallization of PVA is decreased. For tourmaline, the OH groups located at 3626 and 3561 cm^{-1} are distributed into two different sites: Y and Z cation sites [22]. These characteristic bands have disappeared after the reaction and other absorption bands can still be observed, meaning that these reactive OH groups may be involved in the polymerization. The presence of carboxylate group is testified by the absorption bands at 1565 cm^{-1} and 1409 cm^{-1}, attributing respectively to the asymmetrical and symmetrical stretching of carboxylate group. For the composite, no new absorption bands are found, implying that PVA semi-IPN, rather than PVA grafted PAA/Tm composite has been formed successfully.

3.2. DSC analysis

DSC curves of PVA, PAA/Tm and PVA semi-PAA/Tm are shown in Fig. 2. It is observed that these three samples show maximum endothermic peaks at 245, 424 and 423 °C, respectively. The maximum endothermic peak of PVA/PAA/Tm composite lies between

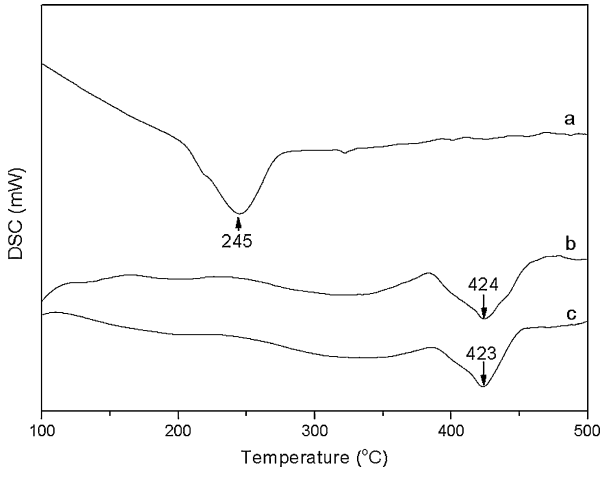

Fig. 2. DSC curves of (a) PVA, (b) PAA/Tm, and (c) PVA semi-IPN PAA/Tm composite.

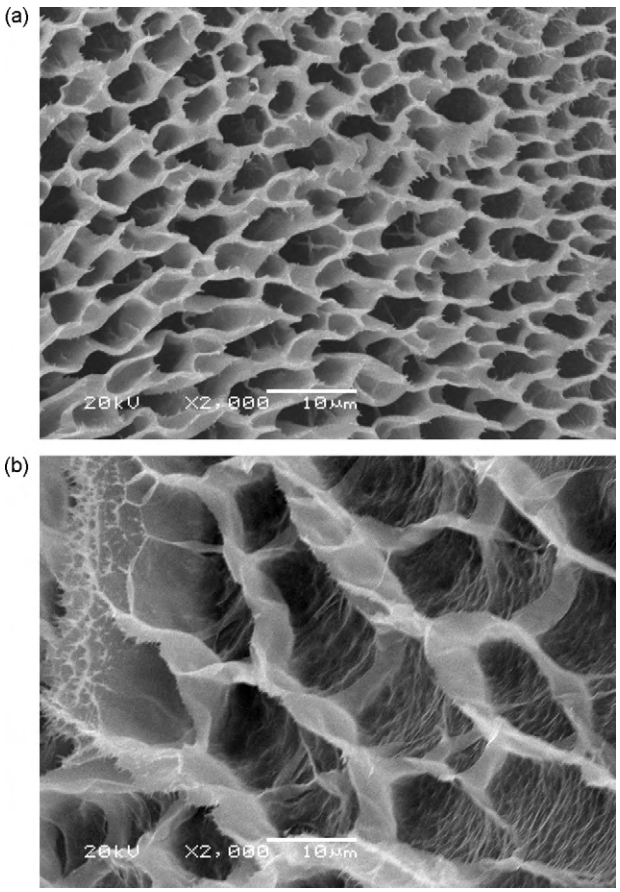

Fig. 3. SEM micrographs of PAA/Tm (a) and PVA semi-IPN PAA/Tm (b) composites.

those of the two native compounds, suggesting its semi-IPN structure. This endothermic peak is close to that of PAA/Tm as a result of lower PVA content in the composite. It is this that the thermal stability of PVA semi-PAA/Tm is not affected by PVA introduction. Zheng et al. investigated the properties of semi-IPN poly(acrylic acid)/Ca-bentonite/poly(dimethyldiallylammonium chloride) and concluded similar results [23].

3.3. SEM analysis

SEM is the most widely employed technique to investigate the shape, size, and porosity of the hydrogels [24,25]. In the present study, we used this technique to identify the differences in the surface morphology of PAA/Tm and PVA semi-IPN PAA/Tm composite, as shown in Fig. 3. It is observed that the two hydrogels have similar three-dimensional pores which are interconnected each other, but some differences can still be visible. PAA/Tm shows a well structured three-dimensional network while PVA semi-IPN PAA/Tm exhibits some pores with thick, compact walls on the surface. This is expected to be orderly aggregates of polymer chain segments in the inner of the semi-IPN hydrogel. During the experiment, we have found that the incorporation of PVA into PAA/Tm can decrease the swelling ratio of corresponding hydrogel, and SEM analysis is consistent with this finding. In other words, the introduction of PVA into the PAA/Tm composite can form some thick, compact walls compared to the original one and thus cannot afford facilities for the entrance of water molecules, leading the lower swelling ratio of PVA semi-IPN PAA/Tm than that of PAA/Tm. The lower swelling ratio is considered to be more desirable for the adsorption technology.

3.4. Optimization of preparation parameters for PVA semi-IPN PAA/Tm

As can be seen from Table 2, there was a considerable difference in the adsorption capacity for Pb^{2+} and Cu^{2+} removal at different value of selected parameters. The coefficient of the model for the response was estimated using multiple regression analysis method based on Eq. (2). The empirical relationship between adsorption capacity for heavy metals and three test variables in coded units is given by

$$Y_{Pb}^{2+} = 2.95 + 0.46x_1 + 0.07x_2 - 0.22x_3 - 0.29x_1x_2 - 0.10x_1x_3 - 0.14x_2x_3 - 0.30x_1^2 - 0.058x_2^2 - 0.36x_3^2 \quad (4)$$

$$Y_{Cu}^{2+} = 2.87 + 0.51x_1 + 0.024x_2 - 0.24x_3 - 0.27x_1x_2 - 0.017x_1x_3 + 0.012x_2x_3 - 0.61x_1^2 - 0.26x_2^2 - 0.79x_3^2 \quad (5)$$

where Y is the adsorption capacity for Pb^{2+} or Cu^{2+} in mmol/g, x_1, x_2, and x_3 are the coded values of the test variables, ND of AA (x_1), PAV:AA ratio (x_2) and Tm:AA (x_3). The results in term of analysis of variance (ANOVA) for Eqs. (4) and (5) are summarized in Tables 3 and 4. The significant of each coefficient was determined by F value and P value. The larger the value of F and the smaller the value of P, the more significant is the corresponding coefficient term [26,27]. The results show that the regressions for removing Pb^{2+} and Cu^{2+} are statistically significant with F value of 4.78 and P value of 0.0256 for Pb^{2+} removal and F value of 196.62 and P value <0.0001 for Cu^{2+} removal. By analyzing the F value and P value, it is observed that x_1 and x_3^2 are the significant model terms for Pb^{2+} removal, while for Cu^{2+} removal, x_1, x_3, x_1x_2, x_1^2, x_2^2 and x_3^2 are the significant terms. The fit of these models can be checked by the determination coefficient R^2. It is clearly observed from Tables 3 and 4 that

Table 3
ANOVA for response surface quadratic model for preparation variables for removing Pb^{2+}.

Source	Sum of squares	Degrees of freedom	Mean squares	F value	P value Prob > F
Model	3.60	9	0.400	4.78	0.0256
x_1	1.70	1	1.70	20.3	0.00280
x_2	0.0390	1	0.0390	0.470	0.517
x_3	0.396	1	0.396	4.74	0.0660
x_1x_2	0.328	1	0.328	3.92	0.0881
x_1x_3	0.0422	1	0.0422	0.500	0.500
x_2x_3	0.0798	1	0.0798	0.950	0.361
x_1^2	0.385	1	0.385	4.61	0.0690
x_2^2	0.0144	1	0.0144	0.170	0.691
x_3^2	0.543	1	0.543	6.49	0.0383
Residual	0.586	7	0.0836		
Corrected total	4.18	16			

R^2, 0.8601; adjusted R^2, 0.6802; CV, 11.1.

Table 4
ANOVA for response surface quadratic model for preparation variables for removing Cu^{2+}.

Source	Sum of squares	Degrees of freedom	Mean squares	*F* value	*P* value Prob > *F*
Model	7.75	9	0.862	197	$<1.00 \times 10^{-4}$
x_1	2.08	1	2.08	474	$<1.00 \times 10^{-4}$
x_2	4.62×10^{-3}	1	4.62×10^{-3}	1.05	0.339
x_3	0.458	1	0.458	105	$<1.00 \times 10^{-4}$
x_1x_2	0.300	1	0.300	68.4	$<1.00 \times 10^{-4}$
x_1x_3	1.14×10^{-3}	1	1.14×10^{-3}	0.260	0.625
x_2x_3	6.18×10^{-4}	1	6.18×10^{-4}	0.140	0.718
x_1^2	1.54	1	1.54	352	$<1.00 \times 10^{-4}$
x_2^2	0.286	1	0.286	65.4	$<1.00 \times 10^{-4}$
x_3^2	2.66	1	2.66	606	$<1.00 \times 10^{-4}$
Residual	0.0307	7	4.38×10^{-3}		
Corrected total	7.78	16			

R^2, 9961; adjusted R^2, 0.9910; CV, 3.16.

compared with Pb^{2+} removal ($R^2 = 0.8601$), the value of the determination coefficient for Cu^{2+} removal ($R^2 = 0.9961$) is higher. At the same time, the higher adjusted determination coefficient (adjusted $R^2 = 0.9910$) and a relatively low value of the coefficient of variation (CV = 3.16) support a high significance of corresponding model for Cu^{2+} removal and good precision and reliability of the experiments [28]. Though the determination coefficient for Pb^{2+} removal ($R^2 = 0.8601$) is not as high as that for Cu^{2+} removal, it can predict well the response for the current model. The predicted *q* versus actual *q* plots for Pb^{2+} and Cu^{2+} removal are shown in Fig. 4. The observed points on both of these plots reveal that the actual values are distributed relatively near to the straight line in both cases.

The 3D surface graphs for Pb^{2+} and Cu^{2+} removal are shown in Fig. 5. Pb^{2+} and Cu^{2+} removal shows to be very sensitive to the changes in ND of AA and Tm:AA, while PVA:AA has insignificant effects for the adsorption capacity. Generally, a low amount of clay into the hydrogel can improve the polymeric networks [29], and thus is responsible for higher adsorption capacity. Similar observation had also been reported by Kaşgöz et al. [3]. Increase in ND of AA can produce a large amount of negatively charged $-COO^-$ groups which are expected to increase the number of available adsorption sites for Pb^{2+} and Cu^{2+} ions. The high degree of deprotonation of these binding groups can thus improve its adsorption capacity for heavy metals. By numerical optimization, we can obtain the optimal preparation conditions for PVA semi-IPN PAA/Tm composite with highest adsorption capacity for Pb^{2+} and Cu^{2+} removal: ND of AA = 68–69%, PVA:AA = 0.0973, Tm:AA = 0.20. Based on above discussions, it can be concluded that RSM can not only afford the optimum values of studied factors, but also give valuable information on the adsorption mechanism.

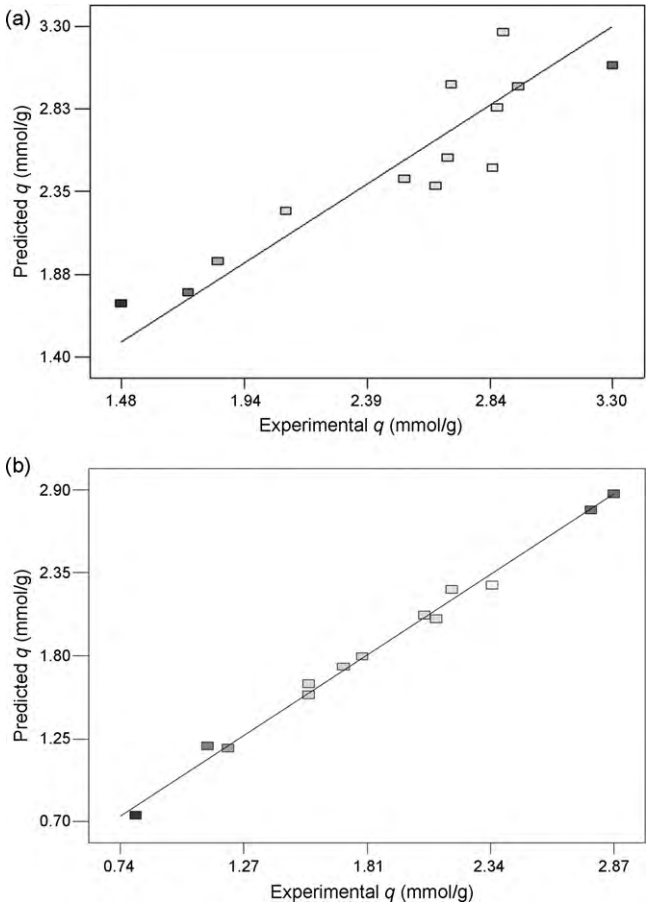

Fig. 4. Comparison plots between the experimental and model predicted Pb^{2+} (a) and Cu^{2+} (b) adsorption capacity.

3.5. Adsorption studies

Preliminary experiments indicated that the adsorption of Pb^{2+} and Cu^{2+} onto as-prepared composite occurred rapidly and the adsorption equilibrium could be achieved within 30 min (Fig. 6). This faster adsorption kinetics is correlated with the structure of the composite. PVA semi-IPN PAA/Tm is a three-dimensional structured polymer hydrogel containing lots of super-hydrophilic carboxyl and carboxylate groups, which are considered as the adsorption sites for heavy metals. Due to the super-hydrophilic characteristic, this composite would be swollen quickly when contacting with aqueous solution by which the carboxyl and carboxylate groups present within the polymeric networks can capture these heavy metals. When the adsorption equilibrium is achieved, the adsorption capacities of this composite prepared under the optimum conditions are 3.12 mmol/g for Pb^{2+} and 2.98 mmol/g for Cu^{2+}, as listed in Table 5. These values are in agreement with the predicted values, 3.18 mmol/g for Pb^{2+} and 3.00 mmol/g for Cu^{2+}, suggesting that Eqs. (4) and (5) are valid for predicting Pb^{2+} and Cu^{2+} adsorption.

During the adsorption, ion exchange and chelation coexist, as shown in Eqs. (6) and (7):

$$RCOOH \leftrightarrow RCOO^- + H^+ \quad (6)$$

$$2RCOO^- + M^{2+} \leftrightarrow (RCOO)_2M \quad (7)$$

where M denotes Pb^{2+} or Cu^{2+} ion. The presence of ion exchange can be testified by checking the pH values before and after the adsorption. During the experiment, the pH value exhibits a decreasing tendency with prolonging the contact time, and this is ascribed to the dissociation of carboxyl groups, as shown in Eq. (6).

In order to further illustrate the adsorption mechanism of as-prepared composite for Pb^{2+} and Cu^{2+}, Fig. 7 represented the FTIR

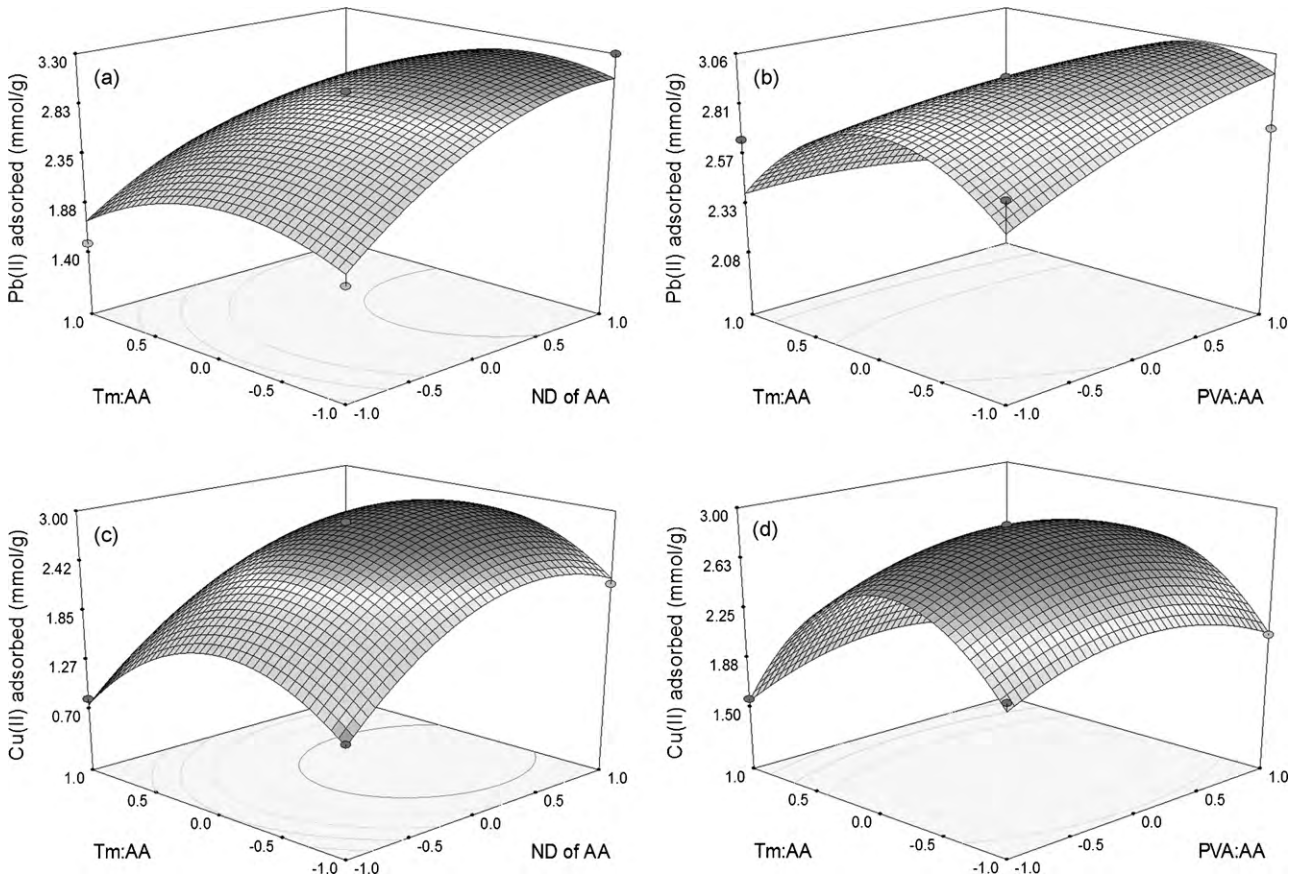

Fig. 5. Response surface plots for the effect of (a) ND of AA and Tm:AA, and (b) PVA:AA and Tm:AA on Pb^{2+} removal; (c) ND of AA and Tm:AA, and (d) PVA:AA and Tm:AA on Cu^{2+} removal. Adsorption experiments: initial concentration C_0, 0.02 mol/L; adsorbent dose, 50 mg/25 mL; natural pH; 30 °C/120 rpm; 1.5 h.

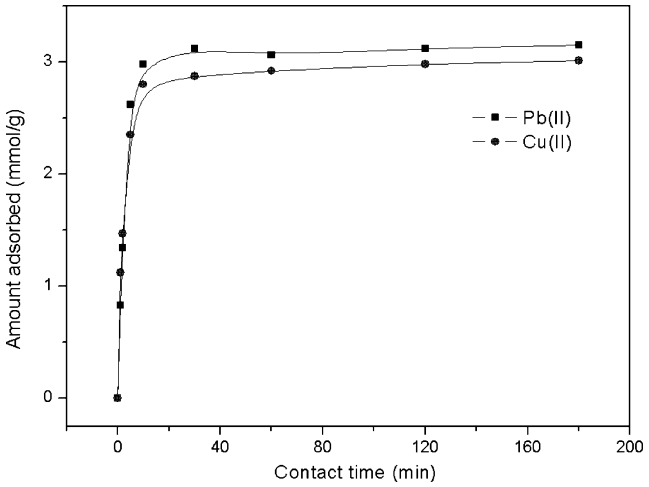

Fig. 6. Adsorption capacity as a function of contact time in non-competitive conditions. Adsorption experiments: C_0, 0.02 mol/L; adsorbent dose, 50 mg/25 mL; natural pH; 30 °C/120 rpm.

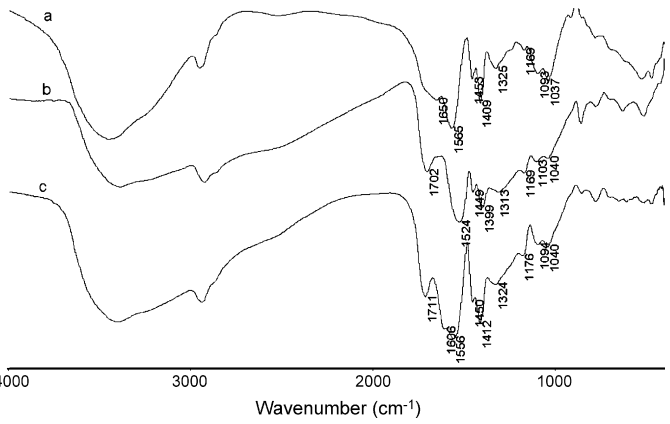

Fig. 7. Infrared spectra of PVA semi-IPN PAA/Tm before (a) and after adsorption for Pb^{2+} (b) and Cu^{2+} (c).

Table 5
Optimized preparation variables for Pb^{2+} and Cu^{2+} adsorption through point prediction method.

ND of AA	PVA:AA	Tm:AA	Pb^{2+} adsorbed (mmol/g)		Cu^{2+} adsorbed (mmol/g)	
			Predicted	Experimental	Predicted	Experimental
68–69%	0.0973	0.20	3.18	3.12	3.00	2.98

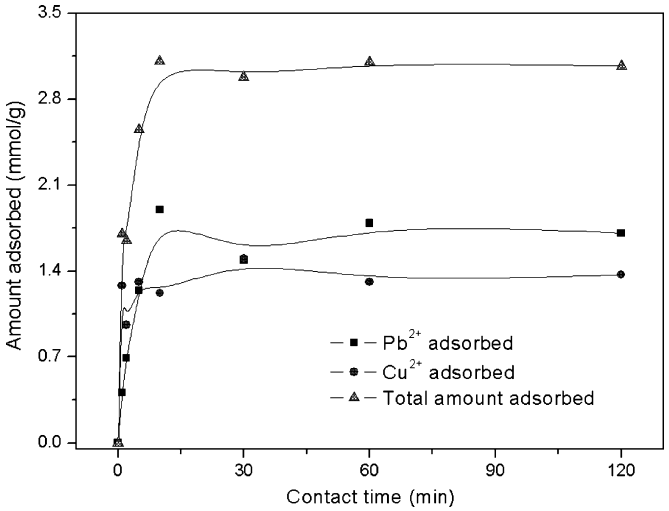

Fig. 8. Plots of adsorbed metal ion amounts by PVA semi-IPN PAA/Tm composite in competitive conditions. Adsorption experiments: C_0, 0.01 mol/L; adsorbent dose, 50 mg/25 mL; natural pH; 30 °C/120 rpm.

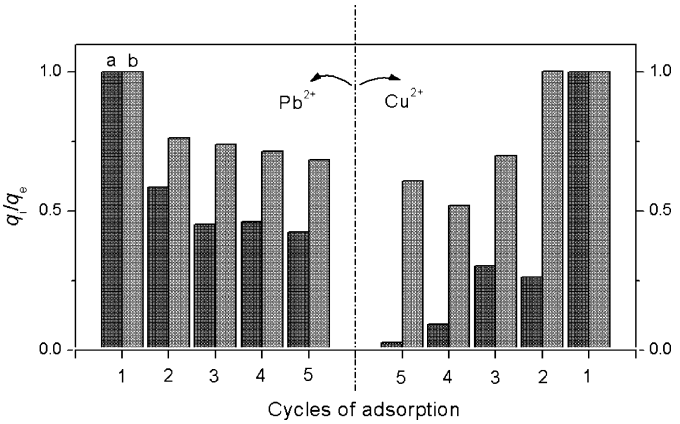

Fig. 9. Reusable ability of PVA semi-TPN PAA/Tm composite. (a) 0.1 mol/L HCl as the desorbing agent, and (b) 0.1 mol/L EDTA as the desorbing agent.

spectra of PVA semi-IPN PAA/Tm before and after the adsorption. The results indicate that the vibration band of asymmetric vibration absorption (ν_{asCOO}) of carboxylate group in the composite has shifted from 1565 cm^{-1} to lower wavenumbers of 1524 cm^{-1} and 1556 cm^{-1} for Pb^{2+} and Cu^{2+} adsorption, respectively, and the vibration band of symmetric vibration absorption (ν_{sCOO}) of carboxylate group in the composite is similar to that of composite before adsorption. This is the result of coordination of carboxylate to Pb^{2+}/Cu^{2+} ions. Generally, a large splitting of –COO stretching frequency ($\nu_{asCOO}-\nu_{sCOO}$) is often an indication of monodentate coordination, while a similar splitting of –COO stretching frequency is considered to be bidentate chelate [30]. In this study, the splitting of –COO stretching frequency after the adsorption is not different greatly from the free ion spectrum (Fig. 7a), suggesting that the carboxylate group in the composite acts as a bidentate chelate. In addition, the absorption bands lying at 1325 cm^{-1} (related to the hydroxyl group) and 1093 cm^{-1} associated with the vibration of C–O have shifted to lower wavenumber of 1313 cm^{-1} and higher wavenumber of 1103 cm^{-1} after adsorption for Pb^{2+} ion, while for Cu^{2+} adsorption, these absorption bands are not far away with those before adsorption. The information implies that –OH groups derived from PVA have participated in the coordination with Pb^{2+}, but has no contribution to the coordination with Cu^{2+}, which may cause the differences in the adsorption capacity for Pb^{2+} and Cu^{2+} removal. Furthermore, carboxyl groups lying at around 1702 cm^{-1} is enhanced obviously, another evidence of the presence of ion exchange during the adsorption process.

Adsorption capacities of the optimum composite were also investigated in a mixed solution containing Pb^{2+} and Cu^{2+} ions. Dependence of the metal ion adsorption capacities on the contact time is represented in Fig. 8. It can be seen that high adsorption rate is observed at the beginning and the adsorption saturation is achieved within 10 min. It seems that at the beginning, the composite shows a stronger binding affinity for Cu^{2+} ion, thereafter, with prolonging the contact time, a larger amount of Pb^{2+} ion is adsorbed by this composite. Nevertheless, the total amount adsorbed for Pb^{2+} and Cu^{2+} is found to be 3.10 mmol/g, approximating to that for single Pb^{2+} or Cu^{2+} adsorption with the same initial concentration.

3.6. Desorption and reusability

Adsorption is a well established technology for water and wastewater purification. However, the success of this technology, for environmental and economic reasons, depends on the possibility of desorbing the target contaminant and reusing the adsorbent. HCl and EDTA are important desorbing agents for recovering the adsorbent used for heavy metals removal [4,31]. In this study, metal ion adsorbed composite was treated with 0.1 mol/L HCl or EDTA solution as described in the experimental part. When the spent adsorbent was recovered, the reusability was evaluated, as shown in Fig. 9. The results indicate that the metal ions adsorbed can be desorbed efficiently by 0.1 mol/L EDTA solution. Though the adsorption capacity for Pb^{2+} and Cu^{2+} is observed to decrease with increasing the cycles of adsorption, it can adsorb more Pb^{2+} and Cu^{2+} ions with higher q_i/q_e, where q_i and q_e denotes respectively the adsorption capacity of each cycle and the first equilibrium adsorption capacity. The adsorption/desorption tests reveal that PVA semi-IPN PAA/Tm composite is an efficient adsorbent for Pb^{2+} and Cu^{2+} removal.

4. Conclusions

RSM enables to estimate all linear and quadratic effects and 2-factor interactions, and requires less runs compared to conventional time-consuming experimental methods. In this study, RSM based on three-factor-three-level BBD was firstly used to optimize the preparation variables of PVA semi-IPN PAA/Tm according to the adsorption capacity for Pb^{2+} and Cu^{2+} ions. By fitting the empirical models, the maximum Pb^{2+} and Cu^{2+} removal can be achieved under these conditions: ND of AA, 68–69%; PVA:AA ratio, 0.0973; Tm:AA ratio, 0.20. RSM can afford the valuable information about the experimental variables, predict the experimental results, and also give some clues about the adsorption mechanism which may in turn guide the experimental process. Adsorption kinetic studies reveal that the adsorption equilibrium can be achieved within 30 min with higher adsorption capacity of 3.12 mmol/g for Pb^{2+} ion and 2.98 mmol/g for Cu^{2+} ion. These metal ions can be effectively desorbed by 0.1 mol/L EDTA solution and the recovered composite can be used again to adsorb metal ions.

Acknowledgements

This work is supported by the National Natural Science Foundation of China (No. 20877077).

References

[1] T. Bahadir, G. Bakan, L. Altas, H. Buyukgungor, The investigation of lead removal by biosorption: an application at storage battery industry wastewaters, Enzyme Microb. Technol. 41 (2007) 98–102.

[2] K. Kadirvelu, K. Thamaraiselvi, C. Namasivayam, Removal of heavy metals from industrial wastewaters by adsorption onto activated carbon prepared from an agricultural solid waste, Bioresource Technol. 76 (2001) 63–65.
[3] H. Kaşgöz, A. Durmuş, A. Kaşgöz, Enhanced swelling and adsorption properties of AAm-AMPSNa/clay hydrogel nanocomposites for heavy metal ion removal, Polym. Adv. Technol. 19 (2008) 213–220.
[4] X. Wang, Y. Zheng, A. Wang, Fast removal of copper ions from aqueous solution by chitosan-g-poly(acrylic acid)/attapulgite composites, J. Hazard. Mater. 168 (2009) 970–977.
[5] S.-H. Huang, D.-H. Chen, Rapid removal of heavy metal cations and anions from aqueous solutions by an amino-functionalized magnetic nano-adsorbent, J. Hazard. Mater. 163 (2009) 174–179.
[6] Y. Zheng, P. Li, J. Zhang, A. Wang, Study on superabsorbent composite XVI. Synthesis, characterization and swelling behaviors of poly(sodium acrylate)/vermiculite superabsorbent composites, Eur. Polym. J. 43 (2007) 1691–1698.
[7] A. Li, A. Wang, J. Chen, Studies on poly(acrylic acid)/attapulgite superabsorbent composite. I. Synthesis and characterization, J. Appl. Polym. Sci. 92 (2004) 1596–1603.
[8] F. Santiago, A.E. Mucientes, M. Osorio, F.J. Poblete, Synthesis and swelling behaviour of poly (sodium acrylate)/sepiolite superabsorbent composites and nanocomposites, Polym. Int. 55 (2006) 843–848.
[9] C.C. DeMerlis, D.R. Schoneker, Review of the oral toxicity of polyvinyl alcohol (PVA), Food Chem. Toxicol. 41 (2003) 319–326.
[10] M.R. Melo-Junior, L.C. Alves, F.B. Santos, E.I.C. Beltrão, L.B. Carvalho Jr., Polysiloxane–polyvinyl alcohol discs as support for antibody immobilization: Ultra-structural and physical–chemical characterization, React. Funct. Polym. 68 (2008) 315–320.
[11] R.R. Yeredla, H. Xu, Incorporating strong polarity minerals of Tourmaline with semiconductor titania to improve the photosplitting of water, J. Phys. Chem. C 112 (2008) 532–539.
[12] D.C. Montgomery, Design and Analysis of Experiments, fifth ed., John Wiley & Sons, New York, 2001.
[13] G.M. Clarke, R.E. Kempson, Introduction to the Design and Analysis of Experiments, Arnold, London, 1997.
[14] J.A. Cornell, How to Apply Response Surface Methodology, second ed., American Society for Quality Control, Wisconsin, 1990.
[15] G. Box, N. Draper, Empirical Model Building and Response Surfaces, John Wiley & Sons, New York, 1987.
[16] C. Cojocaru, G. Zakrzewska-Trznadel, Response surface modeling and optimization of copper removal from aqua solutions using polymer assisted ultrafiltration, J. Membrane Sci. 298 (2007) 56–70.
[17] A. Özer, G. Gürbüz, A. Çalimli, B.K. Körbahti, Biosorption of copper(II) ions on *Enteromorpha prolifera*: application of response surface methodology (RSM), Chem. Eng. J. 146 (2009) 377–387.
[18] J.I.S. Khattar, Shailza, Optimization of Cd^{2+} removal by the cyanobacterium *Synechocystis pevalekii* using the response surface methodology, Process Biochem. 44 (2009) 118–121.
[19] H. Tadokoro, Infrared studies of polyvinyl alcohol by deuteration of its OH groups, B. Chem. Soc. Jpn. 32 (1959) 1252–1257.
[20] H.S. Mansur, R.L. Oréfice, A.A.P. Mansur, Characterization of poly(vinyl alcohol)/poly(ethylene glycol) hydrogels and PVA-derived hybrids by small-angle X-ray scattering and FTIR spectroscopy, Polymer 45 (2004) 7193–7202.
[21] H. Tadokoro, Crystallization-sensitive band of polyvinyl alcohol, Bull. Chem. Soc. Jpn. 32 (1959) 1334–1339.
[22] B.J. Reddy, R.L. Frost, W.N. Martens, D.L. Wain, J.T. Kloprogge, Spectroscopic characterization of Mn-rich tourmalines, Vib. Spectrosc. 44 (2007) 42–49.
[23] L. Zheng, S. Xu, Y. Peng, J. Wang, G. Peng, Preparation and swelling behavior of amphoteric superabsorbent composite with semi-IPN composed of poly(acrylic acid)/Ca-bentonite/poly(dimethyldiallylammonium chloride), Polym. Adv. Technol. 18 (2007) 194–199.
[24] P.S.K. Murthy, Y.M. Mohan, J. Sreeramulu, K.M. Raju, Semi-IPNs of starch and poly(acrylamide-co-sodium methacrylate): Preparation, swelling and diffusion characteristics evaluation, React. Funct. Polym. 66 (2006) 1482–1493.
[25] S. Jin, M. Liu, F. Zhang, S. Chen, A. Niu, Synthesis and characterization of pH-sensitivity semi-IPN hydrogel based on hydrogen bond between poly(N-vinylpyrrolidone) and poly(acrylic acid), Polymer 47 (2006) 1526–1532.
[26] K.M. Helen, R. lyyaswami, G.P. Magesh, R.M. Lima, Modelling, analysis and optimization of adsorption parameters for H_3PO_4 activated rubber wood sawdust using response surface methodology (RSM), Colloid Surf. B 70 (2009) 35–45.
[27] M. Amini, H. Younesi, N. Bahramifar, A.A.Z. Lorestani, F. Ghorbani, A. Daneshi, M. Sharifzadeh, Application of response surface methodology for optimization of lead biosorption in an aqueous solution by *Aspergillus niger*, J. Hazard. Mater. 154 (2008) 694–702.
[28] R.O. Kuehl, Design of Experiments: Statistical Principles of Research Design and Analysis, 2nd ed., Duxbury Press, Pacific Grove, CA, 2000.
[29] Y. Zheng, J. Zhang, A. Wang, Fast removal of ammonium-nitrogen from aqueous solution using chitosan-g-poly (acrylic acid)/attapulgite composite, Chem. Eng. J. 155 (2009) 215–222.
[30] F. Huang, Y. Zheng, Y. Yang, Study on macromolecular metal complexes: synthesis, characterization, and fluorescence properties of stoichiometric complexes for rare earth coordinated with poly(acrylic acid), J. Appl. Polym. Sci. 103 (2007) 351–357.
[31] Y.-T. Zhou, H.-L. Nie, C. Branford-White, Z.-Y. He, L.-M. Zhu, Removal of Cu^{2+} from aqueous solution by chitosan-coated magnetic nanoparticles modified with α-ketoglutaric acid, J. Colloid Interface Sci. 330 (2009) 29–37.